2011 American Control Conference
on O'Farrell Street, San Francisco, CA, USA
June 29 - July 01, 2011

Strategies to Minimize Fuel Consumption of Passenger Cars during Car-Following Scenarios

Shengbo Eben Li and Huei Peng

Abstract— **One of the important factors that affects a vehicle's fuel consumption is how it is driven. For a passenger car with an internal combustion engine and continuous variable transmission, this paper quantitatively identified its fuel-optimal driving operations in car-following scenarios and extracted two useful strategies with implementable profiles, Pulse-and-Gliding (PnG) and Constant Speed (CS). After further analysis, it is concluded that as the preceding vehicle's speed increases, a partial Pulse-and-Gliding, full-Pulse-and-Gliding and Constant Speed strategy becomes optimal successively; and their selection is mainly dominated by both static and transient fueling characteristics of engine. Moreover, in a full-PnG operation, engine always switches between minimum BSFC point and idling point while the range error oscillates between its upper and lower bounds.**

I. Introduction

Today, the concerns for energy security and climate change is leading to increasing interests in vehicle economic techniques. Among all the techniques, one important approach is related to how to manipulate a vehicle [1]. For instance, Leonard [2] found that some skillful drivers are able to save fuel without increasing trip time by properly adjusting the vehicle speed. It was demonstrated that driving styles can change fuel efficiency up to 10% even in a normal traffic flow [3]. Related to this fuel-saving technique, two noticeable efforts are undertaking recently: one is the eco-driving project, largely launched in Europe and Japan [4][5], and the other is economy-oriented longitudinal control[6][7]. The former aims to teach fuel-saving skills through driver education, fuel-gauge feedback, and sustainable monitoring, thus enhancing driver's manipulating level in terms of economy. The latter implements fuel saving skills into automatic control systems in order to achieve more efficient operation than average drivers.

In both projects, a critical prerequisite is to have a firm understanding of fuel saving strategies for given driving situations. Now, the most common way to achieve this is to collect large quantity of experimental data and summarize traits of fuel-efficient drivers. Several eco-driving projects have employed this method and result in various qualitative eco-driving tips, e.g. accelerating moderately, maintaining an even driving pace, eliminating excessive idling, etc[4][5]. In addition, a Pulse-and-Gliding (PnG) strategy is also known to achieve better fuel economy in light traffic, like SAE Supermileage Competition [8]. Its basic idea is to run engine at high power, store kinetic energy in vehicle inertia, and then coast down to a low speed only using that energy (while the engine is off). Compared to steady cruising, 33%~77% of fuel reduction was observed in a 2007 Ford Focus [8].

However, both the "eco-driving tips" and "PnG strategy" above are still qualitative. They can be used to educate drivers, but not suitable for precise implementation in automatic controllers. Furthermore, some of the lessons learned now are at odds to each other. For instance, the PnG must have a high acceleration phase while some fuel-saving tips suggest drivers accelerate moderately. The objective of this paper is to quantitatively identify optimal driving operations in more practical situations, car-following scenarios. Based on the identified operations, we will extract fuel-saving strategies useful for automatic control systems, e.g. adaptive cruise control. Meanwhile, we will also explain some inconsistencies between existing eco-driving strategies, e.g. PnG (switches between high acceleration and coasting) and moderate accelerations.

The rest of this paper is organized as follows. For a passenger car with an internal combustion engine, a simplified car-following model is constructed in section 2. Section 3 defines the optimal control problem for best fuel economy. Section 4 demonstrates the identified optimal driving operations and analyzes their corresponding strategies. Finally, conclusions are given in Section 5.

II. Modeling of Car-Following System

A car-following system usually includes a preceding vehicle (PV) and a following vehicle (FV). In this paper, the FV has a 4-cylinder, 2.0-liter gasoline engine and a continuously variable transmission (CVT). To capture the main dynamics in its longitudinal direction, we assume: (1) all powertrain dynamics, e.g. engine, tyre slip, etc, are ignored; (2) the CVT has a wide gear ratio with equal mechanical efficiency [9], and moreover the ratio is always selected to enable engine to track the optimal BSFC (brake

Manuscript received September 20, 2010. This work was supported by the IAT (China) Auto Technology Co., Ltd. The project is aiming to develop an economy-oriented adaptive cruise control algorithm for passenger cars. This paper contains its first step study, identification of optimal driving operations.

Dr. Shengbo Eben Li is with the Department of Mechanical Engineering, University of Michigan, Ann Arbor, MI 48105 USA. Email:lisb04{at}gmail.com.

Prof. Huei Peng is with the Department of Mechanical Engineering, University of Michigan, Ann Arbor, MI 48105 USA. Phone: 734-934-0352, Email: hpeng{at}umich.edu.

specific fuel consumption) line. Then, we have its longitudinal dynamic model [10]:

$$\frac{i_g i_0 \eta_T}{r_w} T_e = M\dot{v} + C_A v^2 + Mgf \,, \tag{1}$$

where T_e is the engine torque, η_T is the mechanical efficiency of the driveline, i_g is the gear ratio of the transmission, i_0 is the gear ratio of the final gear, v is the speed of the FV, M is the lumped vehicle mass, C_A is the coefficient of aerodynamic drag, g is the gravity coefficient, and f is the coefficient of rolling resistance. Employing a constant-time headway policy ($R_d=\tau_h \cdot v_p+d_0$) [11], the car-following dynamics are expressed as:

$$\begin{aligned} \Delta\dot{R} &= \Delta v - \tau_h a_p \\ \Delta\dot{v} &= \frac{1}{M}\left(C_A v^2 + Mgf\right) - \frac{i_g i_0 \eta_T}{M r_w} T_e + a_p \end{aligned}, \tag{2}$$

where $\Delta R=R-R_d$ is the range error between actual and desired inter-vehicle distances, $\Delta v=v_p-v$ is the speed error between the PV and FV, τ_h is the headway time, a_p is the PV's acceleration.

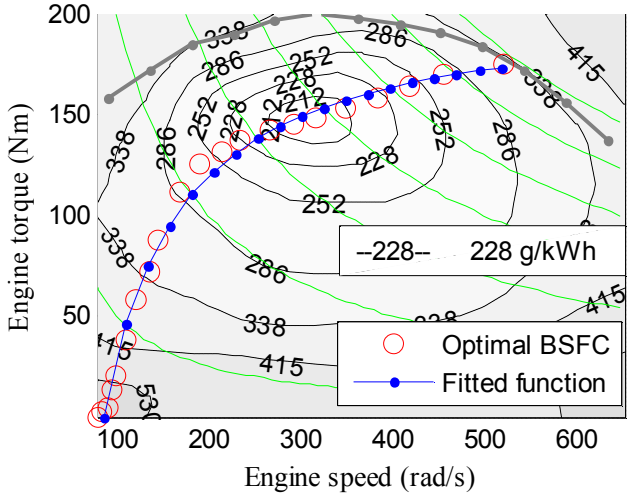

Fig. 1 BSFC characteristics of the gasoline engine

Fig. 1 shows the operating characteristics of the gasoline engine. Its minimum BFSC point is located at about $\omega_e \approx 300$ rad/s and $T_e \approx 150$ m/s. During idling, $\omega_e \approx 100$ rad/s, $T_e = 0$ m/s and a small amount of idling fuel is used to overcome friction and accessory loads. For a typical internal combustion engine, its total fuel consumption can be divided into two components: static fuel and transient fuel. In fuel-saving driving, it is important to consider transient fuel consumption because the engine power may change significantly and frequently. Usually, the static fuel is modeled as the product of engine power and the engine BSFC, while the transient fuel is somewhat complex to describe. Nevertheless, typical transient behaviors of a gasoline engine increase the static fuel consumption by 4~5% [12][13]. To precisely predict engine fuel in this paper, we add a transient correction term to a static fuel model, obtaining:

$$Q_s = q_s + k_e \cdot \dot{T}_e^2 \,, \tag{3}$$

where Q_s is total fuel rate, q_s is the static fuel rate, and k_e is the correcting factor adjustable to compensate for the transient fuel consumption. To estimate the transient correcting coefficient, we assume that the transient fuel consumption should increase static fuel consumption by 4% in the U.S. Federal Test Procedure Cycle FTP-72. Under this assumption, we found $k_e \approx 2.2\times10^{-5}$ g·s^3/(N^2·m^2).

A. *Gear shifting method in CVT*

For the gasoline engine, its optimal BSFC line, indicated by symbols of circles, is shown in Fig. 1. It is fitted by a function OPT(·):

$$\omega_{eopt} = \mathrm{OPT}\left(T_e\right) = \frac{b_{opt}}{1 - k_{opt} \cdot T_e} \,, \tag{4}$$

where ω_{eopt} is the engine speed in the optimal BSFC line, and k_{opt}, b_{opt} are the identified parameters. As assumed before, the gear ratio of the CVT is selected to enable engine track the optimal BSFC line, obtaining:

$$i_g = \frac{r_w}{i_0} \cdot \frac{\omega_{eopt}}{v} \,. \tag{5}$$

Since the powertrain dynamics are all neglected, the engine will operate at the optimal BSFC line all the time by using Eq. (5). This assumption greatly simplifies the numerical optimization of the optimal control problem below.

B. *Analytical Model of engine static fuel rate*

When the gear ratio is selected based on Eq. (5), the static fuel rate q_s is solely a function of the engine power P_e. The static fuel rate for the gasoline engine is shown in Fig. 2 (raw date is derived from Fig. 1).

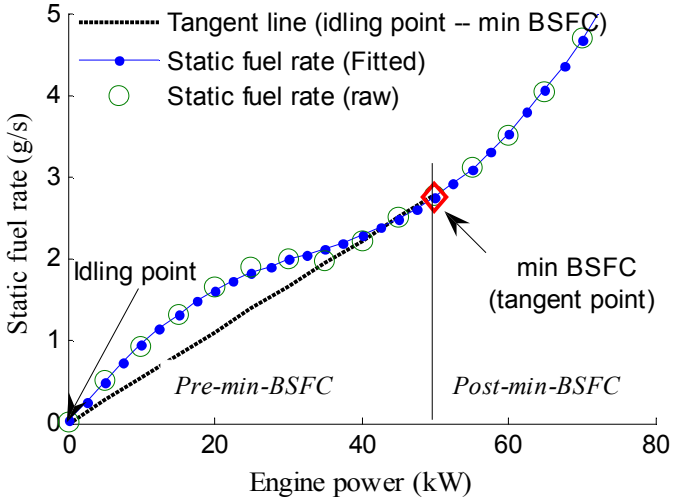

Fig. 2 Static fuel rate of the gasoline engine

To obtain an analytical model, the raw date of the static fuel rate is fitted by a polynomial function (solid-dot line in Fig. 2):

$$q_s = \mathrm{FR}\left(P_e\right) = \sum_{i=0}^{N} k_{FR}\left(i\right) \cdot P_e^i \,, \tag{6}$$

where FR(·) is the polynomial function, $k_{FR}(i)$ are coefficients to be obtained through curve fitting, and N is the degree of the polynomial. We found that N=4 results in adequate accuracy.

Shown as Fig. 2, the static fuel rate of a real engine is nonlinear. In order to interpret its relationship with strategy determining, we draw a tangent line starting from the idling point in Fig. 2. Its tangent point is quiet close to the minimum BSFC point, as diamond point in Fig. 2 (If not strictly exact, the tangent point and minimum BSFC point are alternative.). The tangent point (minimum BSFC point) divides the engine operation into two regions, called pre-min-BSFC region and post-min-BSFC region. In the following, we will demonstrate that the tangent point is critical to select optimal driving operations.

III. Optimal control problem and its numerical optimization

In a car-following situation, range tracking is important. When the range is too large, frequent cut-ins from adjacent lane may occur; when the range is very small, drivers and passengers might felt quite uneasy, and rear-end collisions may happen if the leading vehicle brakes suddenly. In order to avoid these problems, constraints on range error must be imposed:

$$\Delta R_{\min} \le \Delta R \le \Delta R_{\max} \,, \tag{7}$$

where $\Delta R_{\min}$, $\Delta R_{\max}$ are the lower bound and upper bound, respectively. It may be sensible to have $|\Delta R_{\min}|$ smaller than $|\Delta R_{\max}|$ because of humans' sensitivity to collision risks. However, its effect on fuel consumption is negligible. Therefore, we assume that $\Delta R_{\min}$ is always equal to $-\Delta R_{\max}$ in order to reduce the number of free parameters.

To obtain fuel-saving driving strategies, an optimal control problem is constructed to minimize total engine fuel consumption over a horizon $[0, T_f]$:

$$\min J = \int_0^{T_f} Q_s \cdot dt \,, \tag{8}$$

subjecting to the following constraints:

(a) Engine constraints:

$$T_{e\min} \le T_e \le T_{e\max} \,,\ \omega_{e\min} \le \omega_e \le \omega_{e\max} \,,$$

(b) Range constraint: Eq. (7) (9)

(c) Initial and final constraints:

$$\Delta v\left(0\right) = \Delta v\left(T_f\right) = 0,\ \Delta R\left(0\right) = \Delta R\left(T_f\right) = 0 \,.$$

In Eq. (8), T_f is the final time of the problem horizon. In Eq. (9), constraints (a) are hard constraints, imposed by the engine operating limits. Constraints (c) are needed to ensure that the kinetic energy remains identical, and that the total traveling distance of the FV equals that of the PV. TABLE I shows the constraint parameters in the optimal control problem.

TABLE I
CONSTRAINT PARAMETERS IN OPTIMAL CONTROL PROBLEM

Parameter	Value	Parameter	Value
$T_{e\min}$	0 N.m	$T_{e\max}$	170 N.m
$\omega_{e\min}$	80 rad/s	$\omega_{e\max}$	600 rad/s
$\Delta R_{\min}$	-3.0 m	$\Delta R_{\max}$	3.0 m

The optimal control problem is numerically solved by using a commercially available add-on of MATLAB, called GPOPS [14]. GPOPS is based on the so-called Gauss Pseudospectral method, an orthogonal collocation approach. In theory, such a method has the best transcribing accuracy (means high accuracy of solutions) and moreover the resulting nonlinear programming has smaller dimension (means high computing efficiency). A drawback of this approach, as implemented in GPOPS, is that all plant models, cost functions and constraints must be in the form of analytical functions. Fortunately, all the models presented earlier have analytical forms and thus this approach can be used.

IV. Optimization Results and Analysis

In this section, we will perform a series of numerical optimizations to identify optimal control operations. In each optimization, the PV runs at a constant speed. But in different identification the speed is different, ranging from 5m/s to 45m/s. The FV is supposed to largely follow the PV, but has some wiggle room as specified by Eq. (7). The range error (ΔR) constraint is fixed at $\Delta R_{\max}$= $-\Delta R_{\min}$ =3m. In all identification, the problem horizon is 100 seconds.

In addition, because of initial and final constraints imposed by Eq. (9), the behaviors toward either sides of the horizon are somewhat skewed and less insightful. Therefore, we only focus on the middle part of the horizon when analyzing solutions.

A. Optimal driving operations at different PV's speeds

Fig. 3 shows the optimal control operations at v_p=5m/s, 25m/s and 45m/s.

When v_p is 45m/s, the constant speed (CS) strategy is found to be the best. When v_p is 25m/s, however, the Pulse-and-Gliding (PnG) strategy is optimal. In such a strategy, the engine torque switches between the minimum BSFC point (T_e≈150 N.m) and the idling point (T_e≈0 N.m). The range oscillates between its upper and lower bounds. We will refer this maneuvers that alternate between minimum BSFC operation and engine idling as full Pulse-and-Gliding (full-PnG) strategy. When v_p reduces to 5m/s, a full-PnG method is no longer optimal because of the transient fuel penalty in engine. However, a PnG-like maneuver with smoother engine torque emerges, which we call partial-Pulse-and-Gliding (partial-PnG) strategy. In such a strategy, speed and range still fluctuate, but engine never reaches the minimum BSFC point.

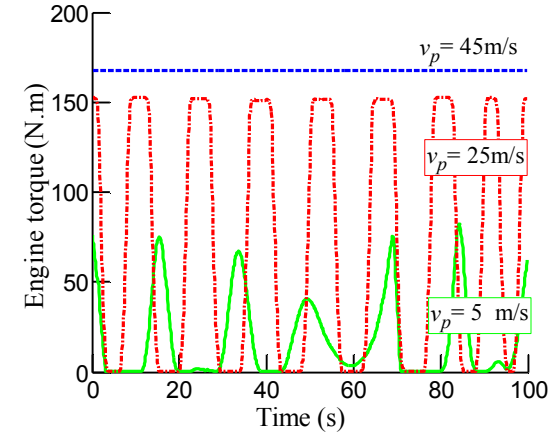

(a) Engine torque of the FV at different PV's speeds

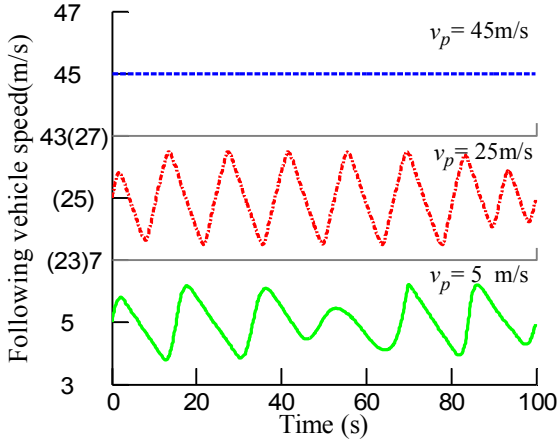

(b) Speed error between the FV and PV

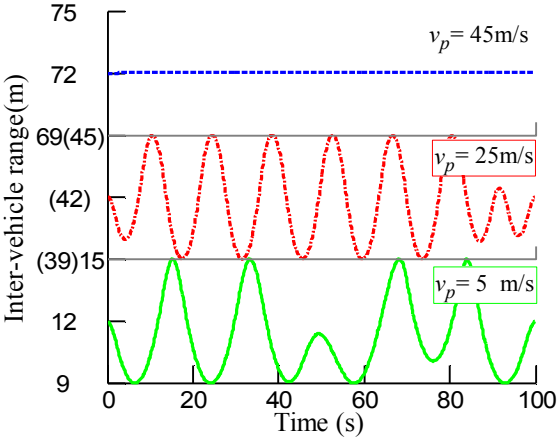

(c) Range error at different PV's speeds

Fig. 3 Optimal fuel saving behavior at different preceding vehicle's speeds

B. *Causes for speed-dependent fuel-saving strategies*

Now, we observed three different optimal driving strategies, i.e., partial-PnG, full-PnG and CS. As indicated by Chang, the quadratic aerodynamic drag is dominating in strategy selection if a vehicle is assumed to have an engine with completely flat BSFC map[15]. The domination is because any fluctuation of speed will cause higher aerodynamic drag, thus consuming more kinetic energy.

However, for a vehicle with internal combustion engine, the strategy is mainly dominated by (a) static fuel rate; and (b) transient fuel rate. As illustrated in Fig. 2, the static fuel rate of a real engine can be divided into two regions, pre-min-BSFC and post-min-BSFC. Their separation occurs at the tangent point (or the minimum BSFC point). To explain the cause of those speed-dependent strategies, we draw a conceptual graph of static fuel rate (Fig. 4).

Neglecting powertrain dynamics, the engine always responds instantaneously to driving operations, and with a CVT it only operates on the optimal BSFC line (corresponding to the static fuel rate line in Fig. 4). Accordingly, a full-PnG operation can be graphically represented by a unique secant line *IT*, of which two endpoints *I*, *T* mean the engine operating points and the dash line between them means the "switching" action. Similarly, a CS operation corresponds to a fixed point *C* in Fig. 4. In addition, we define two other common operations: (1) two-point switching, shown as line *AB* (engine switches between two arbitrary endpoints *A* and *B*); (2) two-point sliding, which is the arc *ACB* (engine slides continuously in a smoothing arc *ACB*, not exceeding endpoints *A* and *B*). It must be noted that the two-point sliding approximates any smoothing operations by a driver or an automatic driving system.

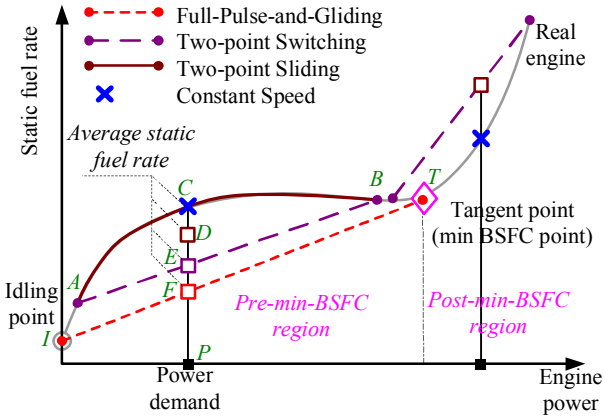

Fig. 4 Conceptual graph of various driving operations and their average static fuel consumption

As shown in Fig. 4, for a given power demand, the average static fuel rate in the two-point switching operation is at point *E* (the intersection between line *AB* and power demand line *CP*). Those of the full-PnG and CS are at *F* and *C*, respectively. That for the two-point sliding operation is a certain point *D* between points *C* and *E*, depending on the sliding maneuver. It is evident that the switching operation always acts more economically than the sliding operation with identical endpoints; further, the full-PnG operation achieves minimum fuel economy because its corresponding graphic line (line *IT*) is lowest among all "feasible" secant lines in static fuel rate curve (Note: "feasible" is defined as a secant line having the power demand line *CP* in between its

two endpoints. Only "feasible" secant lines are possible to provide an average power equal to the power demand.). In other words, when the power demand is in the pre-min-BSFC region, the full-PnG strategy is always optimal if not considering transient fuel penalty.

However, when the PV's speed goes down, the required power also reduces and consequently the fuel improvement from full-PnG decreases. Once the fuel improvement is lower than the transient fuel penalty, the full-PnG operation loses its optimality. The partial-PnG operation, which can reduce transient fuel by smoothing engine behaviors, becomes better.

When the PV's speed is very high, the power demand lies in the post-min-BSFC region. The static fuel rate curves upwards. In Fig. 4, for any power demand in the right of the tangent point, a fixed point is always lowest among all "feasible" secant lines. Therefore, neither switching nor sliding operations are better than a steady operation, thus the CS strategy is optimal.

C. *Changes of duty cycle in full-PnG strategy*

The full-PnG strategy is important because it covers a large portion of driving operations on expressways. Fig. 5 shows the optimal engine torque profiles at several medium speeds. To quantify the torque profiles, we define a duty cycle percentage (λ_{png}) based on the percentage of time when the torque stays at the high level. As can be seen in Fig. 5, λ_{png} increases with the PV's speed, because the power needed to overcome the road load increases.

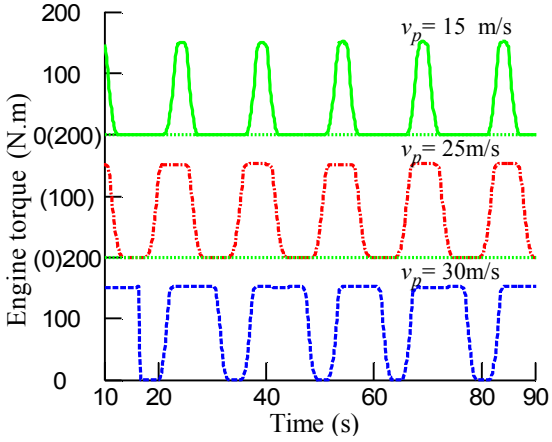

Fig. 5 Optimal engine operations at several medium PV's speeds—all exhibit full-PnG behavior

When the full-PnG strategy is used, the engine switches between two points, but the average power must be equal to the required power. So, λ_{png} can be estimated from the ratio between power demand (P_{edes}) and power at the minimum BSFC point ($P_{e\min}$):

$$\lambda_{PnG} \approx \frac{P_{edes}}{P_{e\min}} \times 100\%, \quad P_{edes} < P_{e\min}$$
$$P_{edes} = \frac{1}{\eta_T}\left(C_A \cdot v_p^3 + Mgf \cdot v_p\right) \qquad (10)$$

Fig. 6 shows the relationship between the static fuel rate, PnG duty cycle and vehicle speed. The left axis corresponds to the complementary duty cycle (1-λ_{png})×100%, where the identified λ_{png} (dot-solid line) is from the optimization results and the calculated λ_{png} (circles) is calculated from Eq.(13). It can be seen that Eq. (10) predicts the PnG duty cycle quite accurately. When the complimentary duty cycle 1-λ_{png} is close to 100% (at 5m/sec and below), we have a partial-PnG strategy which is hard to implement because of its transient nature. When 1-λ_{png}=0%, the CS strategy can be used as a reasonable alternative.

In theory, the separation between full-PnG and CS happens exactly at the speed corresponding to the tangent point (minimum BSFC point). The numerical results however indicate it happens at a slightly lower speed (35m/s, instead of 38m/s) because of the transient fuel penalty.

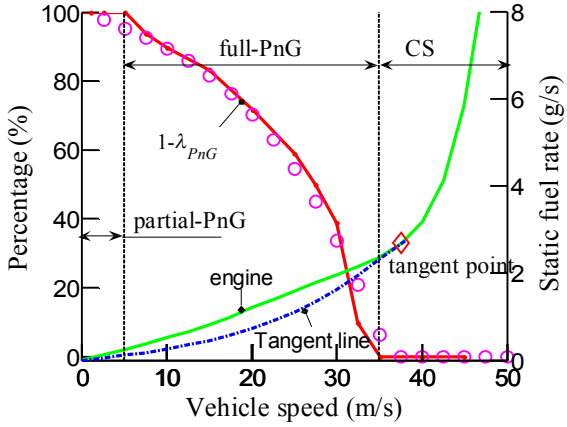

Fig. 6 Relationship between PnG duty cycle and static fuel rate

D. *Fuel economy improvement due to full-PnG*

Compared to steady speed operations, the fuel economy improvement using the full-PnG strategy ascribes to two variables: (a) Duty cycle percentage (λ_{png}) and (b) BSFC benefit (C_{bsfc}). The former reflects the time length that engine works at minimum BSFC point and the latter is the difference between the minimum BSFC point and other point at the required road load, calculated from:

$$C_{bsfc} = \frac{\mathrm{q}_{\mathrm{BSFC}}\left(P_{edes}\right) - \mathrm{q}_{\mathrm{BSFC}}\left(P_{e\min}\right)}{\mathrm{q}_{\mathrm{BSFC}}\left(P_{e\min}\right)} \times 100\% \qquad (11)$$

Increasing either λ_{png} or C_{bsfc} will improve fuel economy of PnG strategy. As illustrated in Fig. 7, λ_{png} increases, but C_{bsfc} decreases with vehicle speed. The fuel economy reaches a maximum of about 32% at 15m/sec, which is roughly half of the speed of minimum BSFC point.

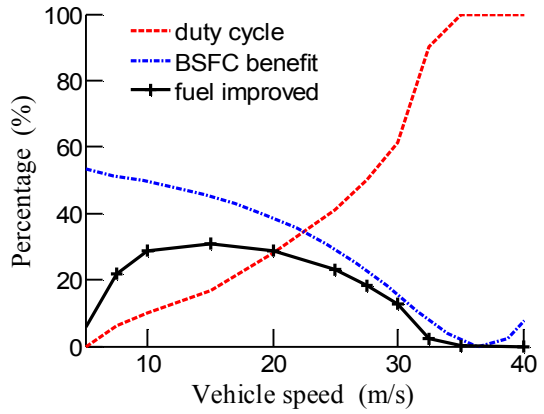

Fig. 7 PnG duty cycle, BSFC benefit and fuel economy improvement vs. preceding vehicle speed

The fuel economy improvement due to the partial-PnG strategy is insignificant. Moreover, it is difficult to implement as a human driving strategy or in automatic control algorithms due to its continuous manipulation. Therefore, in practice, a constant speed approach should be adopted at low speeds (<5m/s). In summary, when designing fuel saving longitudinal control systems, the CS strategy can be used at low and high speeds, and the full-PnG strategy can be used for medium speed. The speed thresholds are vehicle dependent, and for our case they are 5m/sec and 35 m/sec, respectively.

V. Conclusions

This paper analyzed the fuel-optimal driving operations of vehicles in car-following scenarios. We first solve the optimal behavior numerically and then develop implementable algorithms based on the numerical solutions. The major findings include:

1) As average vehicle speed increases, optimal driving maneuver changes from partial Pulse-and-Gliding (PnG), to full Pulse-and-Gliding and finally to Constant Speed (CS) strategy. In reality, however, partial-PnG implementation is difficult and the fuel saving is limited, and thus a CS strategy should be used at both low and high vehicle speeds. In medium speed condition, the full-PnG strategy requires that engine switches periodically between minimum BSFC point and idling point, and the range error oscillates between the upper/lower boundaries.
2) For a passenger car with an internal combustion engine, fuel-optimal driving operations in car-following scenarios are mainly dominated by two factors: (a) engine static fuel rate; and (b) engine transient fuel consumption. The separation threshold of full-PnG and CS is theoretically at the speed corresponding engine minimum BSFC point, but actually somewhat lower because of transient fuel penalty.

Acknowledgment

We highly appreciate Dr. Yuejian Wang in the IAT (China) Auto Technology Co., Ltd for his continuous support on our research work, as well as his valuable advices about how to put our research work into practice. Shengbo Eben Li also thanks Chiao-Ting Li in Dept. of Mechanical Eng., University of Michigan for her help in the earlier work of numerical optimization.

References

[1] J. Barkenbus, "Eco-driving: an overlooked climate change initiative," *Energy Policy*, vol. 38, pp.762–769, 2010.
[2] E. Leonard, "Driver behavior effects on fuel consumption in urban driving," in *Proc. Human Factors Society 22nd Annual Meeting*, vol. 22, no. 6, pp. 438-442, 1978.
[3] R. Marc, "Automobile fuel consumption and emissions: effects of vehicle and driving characteristics," *Annual Review Energy Environment*, vol. 19, pp.75-112, 1994.
[4] B. Beusen, S. Broekx, et al, "Using on-board logging devices to study the longer-term impact of an eco-driving course," *Transportation Research Part D*: *Transport and Environment*, vol. 14, issue 7, 2009, pp. 514-520.
[5] M. Zarkadoula, G. Zoidis, E. Tritopoulou, "Training urban bus drivers to promote smart driving: a note on a Greek eco-driving pilot program," *Transportation Research Part D: Transport and Environment*, vol. 12, issue 6, pp. 449-451, 2007.
[6] S. Li, K. Li, "MPC-based Vehicular Following Control Considering both Fuel Economy and Tracking Capability," in *Proc. of 2008 IEEE VPPC*, Harbin, China, 2008.
[7] C. Manzie, H. Watson, S. Halgamuge, "Fuel economy improvements for urban driving: Hybrid vs. intelligent vehicles," *Transportation Research Part C*:*Emerging Technologies*, vol. 15, issue 1, pp. 1-16, 2007.
[8] J. Lee, D. Nelson, H. Lohse-Busch, "Vehicle Inertia Impact on Fuel Consumption of Conventional and Hybrid Electric Vehicles Using Acceleration and Coast Driving Strategy," in *Proc. of SAE World Cong. & Exhibition*, Detroit, USA, 2009.
[9] R. Pfiffner, L. Guzzella L, C. Onder, "Fuel-optimal control of CVT powertrains," *Control Engineering Practice*, vol. 11, issue 3, pp. 329-336, 2003.
[10] D. Cho, J. Hedrick, "Automotive Powertrain Modeling for Control," *J. Dyn. Sys. Meas. Control*, vol. 111, issue 4, pp. 568-576, 1989.
[11] J. Zhou, H. Peng, "Range Policy of Adaptive Cruise Control Vehicles for Improved Flow Stability and String Stability," *IEEE Trans. on ITS*, vol.6, no.2, pp.229-237, 2005.
[12] S. Lee, *Transient dynamics and control of internal combustion engines*. Beijing: Peoples' Transportation Press, 2001, chap. 3.
[13] C. Ericson, B. Westerberg, R. Egnell, "*Transient emission predictions with quasi stationary models*," SAE International, 2005, no.: 2005-01-3852.
[14] A. Rao, D. Beson, et al, "GPOPS: A MATLAB Software for Solving Multiple-Phase Optimal Control Problems Using the Gauss Pseudospectral Method," *ACM Trans. on Math. Software*, vol. 37, no. 2, 2010.
[15] D. Chang, E. Morlok, "Vehicle Speed Profiles to Minimize Work and Fuel Consumption," J. of Trans. Eng., vol. 131, no. 3, pp. 173-18, 2005.